



Landslide susceptibility mapping by fuzzy gamma operator and GIS, a case study of a section of the national road n°11 linking Mateur to Béja (Nortshern Tunisia)

Adel Klai¹ · Romdhane Haddad¹ · Mohamed Khaled Bouzid¹ · Mohamed Chedly Rabia²

Received: 30 January 2019 / Accepted: 19 December 2019 / Published online: 9 January 2020
© Saudi Society for Geosciences 2019

Abstract

The purpose of this paper is to map the landslide susceptibility using the fuzzy gamma operator and GIS for the section of the national road n°11 linking Mateur to Béja. To minimize the subjectivity of the fuzzy logic approach, the frequency ratio was used to calculate the fuzzy membership. To locate the 147 landslides, Google Earth extracts analysis, and field survey has been done. In this cartography, nine factors controlling landslides were used: slope, aspect, curvature plane, curvature profile, distance to faults, distance to rivers, land use, rainfall, and lithology. Once the fuzziness is calculated in each factor using the frequency ratio (FR), the fuzzy gamma operator can be applied to these nine factors to produce the landslide susceptibility map. Finally, the choice of the nearest susceptibility map of reality is made by applying the ROC curve. By the analysis of the area under curve (AUC), it is seen that the prediction accuracy of model proves that the gamma value of 0.90 yielded the better prediction of landslide susceptibility map (0.89). Finally, our area of interest was classified based on the Jenks natural breaks classification method into five classes, such as non-susceptible zone, low susceptible zone, moderate susceptible zone, high susceptible zone, and very high susceptible zone. Landslide susceptibility mapping based on the fuzzy gamma operator presents a very acceptable result with a reliability of 89%.

Keywords Fuzzy gamma operator · GIS · Landslides · ROC

Abbreviations

AUC	Area under curve
ROC	Receiver operating curves
GIS	Geographic information system
MCDA	Multiple criteria decision analysis
FR	Frequency ratio

Responsible Editor: David Giles

✉ Adel Klai
adelklaiadel@gmail.com

Romdhane Haddad
romdhanhaddad@yahoo.fr

Mohamed Khaled Bouzid
bouzidmohamedkhaled@yahoo.fr

Mohamed Chedly Rabia
rabiamch@gmail.com

¹ Department of Earth Science, Faculty of sciences of Bizerte, University of Carthage, Bizerte, Tunisia

² Department of Geography, Faculty of Letters, Arts and Humanities, University of Manouba, Manouba, Tunisia

Introduction

Landslides are a natural destructive phenomenon that causes material damage, loss of life, and significant damage to natural resources (Intarawichian and Dasananda 2010). This phenomenon represent a major risk for a property, often resulting in loss of life, economic losses, and high maintenance costs (Das et al. 2010). Northern Tunisia and especially the north west of the country suffers from this phenomenon. Marthelot (1957, 1959), Bonvallet (1984a et b) and El Aroui (2016, 2017) have developed a typology of forms caused by landslides and have determined the main causes of their trigger. By determining cause-and-effect relationships, this damage can be mitigated (Intarawichian and Dasananda 2010). The best solution to reduce its damages is to predict the zones of high susceptibility in order to mitigate their consequences. The assesment of the related dangers and susceptibility to the landslide has drawn the attention of both geoscientists and the local authorities (Carrara et al. 1991; Parise 2001; Krejci et al. 2002; Demoulin and Chung 2007; Nefeslioglu et al. 2008). Many technics were proposed in literature for landslide susceptibility mapping (Van Westen 1993; Soeters and Van Westen 1996). According to Feizizadeh and

Blaschke 2012a, b, the GIS-MCDA method is increasingly used in landslide susceptibility mapping for the prediction of future risk areas. However, LSM methods based on GIS-MCDA are often used without any indication of the error rate or confidence in the results. The uncertainty of the results is explained by the large amount of parameters and the heterogeneity of the data sources. Changes in factor weights and decision methods have a significant influence on the ranking order of the criteria and may alter the results (Feizizadeh et al. 2012). In this paper, the fuzzy logic gamma operator has been used to integrate the factors controlling landslides for the first time in Tunisia. We have chosen this method because it is similar to human reasoning, based on linguistic model and for its rapidity operation and its high precision. To minimize the subjectivity of this method, the fuzzy membership values were derived from the frequency ratio of landslides. Then, The fuzzy gamma operator was selected for the integration of causal factors. Finally, to validate the resulting map, ROC curves have been prepared.

Study area

Landslides are well known in Northern Tunisia, which is characterized by steep slopes, heavy rainfall, and fragile lithology. These parameters have a great importance, especially at the level of the watersheds crossed by the national road n°11 that connects the cities of Mateur and Beja. It covers an area of 15,349 ha. Its central value of longitude is 36°55'N, and its latitude is 9°27'E. The altitude varies from 76 to 612 m, and the highest point is located in Jebel Antara. The average annual rainfall and temperature are respectively 650 mm and 17°C. The geology of this region is very complex, and the lithological units include several formations causing landslides. The instability of this area has not been the subject of any mapping study. Often these landslides are very close to the national road n°11, which constitutes a threat for the users of this road. The study location map is illustrated in Fig. 1.

Landslide inventory map

The Landslide inventory map shows mainly the spatial distribution of landslides (Yalcin et al. 2011) and is one of the main steps required to map susceptibility. In this study, the establishment of the inventory map of landslides is based on a Google Earth snippets and field work. A set of 147 landslides was detected in the study area and subsequently digitized for further analysis. Their locations are mapped in Fig. 1. For this analysis, all of the landslides selected were taken for building landslide susceptibility models and after they were used to validate it.

Data preparation

Based on field work and review of previous works, nine factors was determined as primary for the occurrence of landslides, namely, slope, aspect, curvatures, lithology, distance from faults, distance from watercourses, land cover, and rainfall. The Sentinel 2 image with a spatial resolution of 10 m was used to generate the land use map. ALOS PALSAR DEM with a spatial resolution of 12.5 m was used to generate drainage network maps, slope, aspect, and curvatures. Ancillary data such as 1:50000 geological maps and precipitation data were used. All data sets were rasterized in a 10 m × 10 m grid cell. Table 1 shows the different types of data used in this search. When weighting the index cards (qualitative mapping) the choice of the number and the width of the classes consist of a main step because it controls directly the quality of the resulting maps. But in the case of the semi-quantitative mapping that is provided in the present study by the fuzzy logic method, the weight of each class depends on the value of the fuzziness which is estimated from the frequency ratio.

Slope

The slope factor is often used in the development of the landslide susceptibility map because it has a direct effect on the landslide process (Ayalew and Yamagishi 2005; Jordan et al. 2000). Its angle significantly affects the incidence of landslides (Kanungo et al. 2006; Gupta et al. 2008; Dahal et al. 2009). The classification of this parameter is based on previous studies of (Pradhan and Lee 2009; Anbalagan et al. 2015 and Lee et al. 2016). The slope map has six levels: very low/flat (0°–5°), low (5°–10°), moderate (10°–15°), moderately high (15°–20°), high (20°–25°), and very high (> 25°) (Fig. 2).

Aspect

According to DeGraff and Romesburg 1980; Marston et al. 1998; Nagarajan et al. 1998; Saha et al. 2002; Pradhan and Lee 2009; Kanungo et al. 2009; Anbalagan et al. 2015 and Lee et al. 2016 there is a direct relationship between aspect and landslides because humidity and sunshine depend on the exposure of the land. The aspect map was extracted from DEM ALOS PALSAR, it shows nine classes that are; flat (–1), north (0°–22.5° and 337.5°–360°), northeast (22.5°–67.5°), east (67.5°–112.5°), southeast (112.5°–157.5°), south (157.5°–202.5°), southwest (202.5°–247.5°), west (247.5°–292.5°), and northwest (292.5°–337.5°) (Fig. 2).

Rainfall

After heavy rains, the water infiltrates in the soil and increases the degree of saturation which facilitates the triggering of

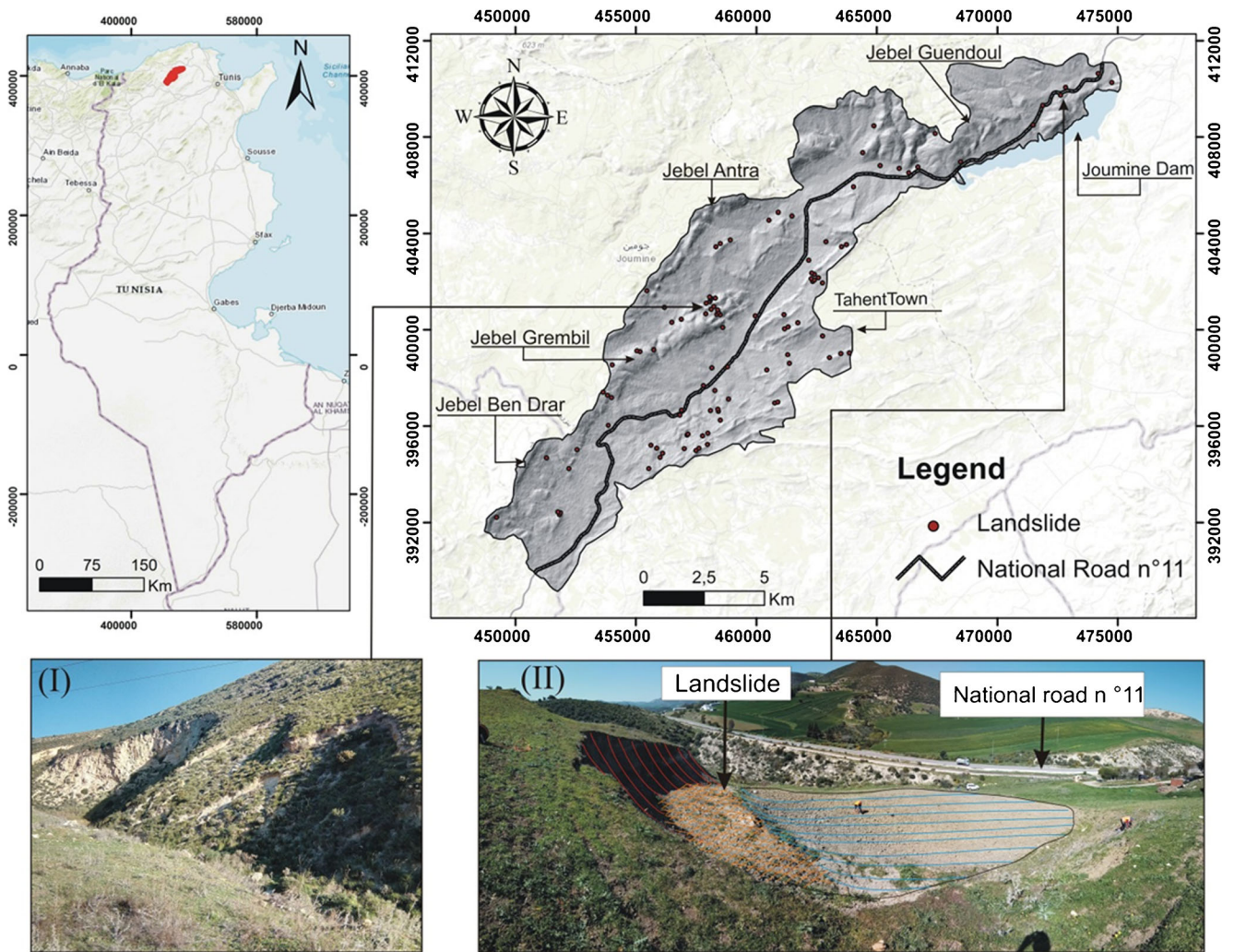


Fig. 1 Location of study area; (I) and (II): examples of landslides characterizing the study area

landslides (Pourghasemi et al. 2009). This factor was prepared on the basis of rainfall data for the period 1982–2012 of rainfall stations of Tebourba, Mateur, Joumine Dam, Ghezala Dam, Bazina, Beja, Sejname delgation and Nefza (rainfall data from the National Institute of Meteorology). In this study, the rainfall map was classified into four classes, < 600, 600–800, 800–1000, and > 1000 mm/year (Fig. 2).

Curvatures

There are two forms of curvature: the profile curvature which is within the direction of the maximum slope and the plan curvature which is perpendicular to the maximum slope direction. In the plan output, a positive curvature indicates that the ground is upwardly convex at this cell. The negative curvature

Table 1 Data used in the present study

Data type	Sensor	Scale	Data derivative
DEM	ALOS PALSAR	12.5 m × 12.5 m grid	Slope Aspect Curvature Distance from the rivers
Image data	Sentinel 2	10 m × 10 m grid	Land use/land cover
Ancillary data	Rainfall data (NIM)	10 m × 10 m grid	Rainfall
Ancillary data	Published geological maps	1/50000	Lithology Distance from the faults

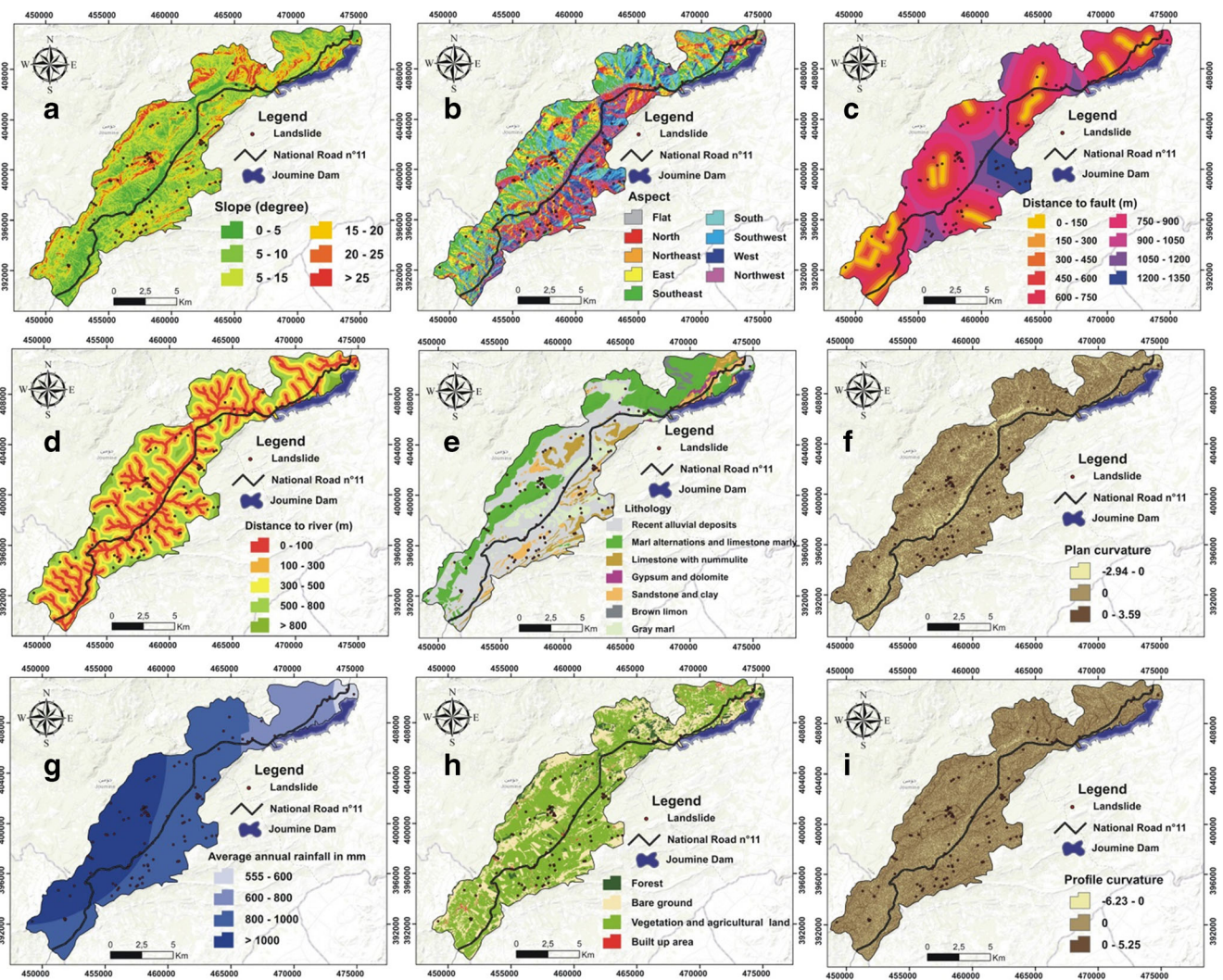


Fig. 2 Input data layers; (A) slope, (B) aspect, (C) distance from the faults, (D) distance from the rivers, (E) lithology, (F) plan curvature, (G) rainfall, (H) land cover, (I) profile curvature

shows that the soil is concave upwardly in this cell. However, in the profile output, it is the opposite, and a value of 0 indicates the ground is flat in both cases (Fig. 2).

Distance from the rivers

The risk of landslides increases with the decreasing of distance from watercourses because they threaten the stability of land by river banks erosion or saturation of materials (Ercanoglu and Gokceoglu 2004). After superimposing the landslides on the hydrographic network, we have noticed that by moving away from watercourses the number of landslides decrease. The distance from river map was prepared by applying the “Euclidean distance” tools under Arcgis 10.2.2. Based on the previous works of (Ilanloo M, 2011 and Wu Y et al. 2016), five levels were determined: very high (< 100 m), high (100–300 m), moderate (300–500 m), low (500–800 m), and very low (> 800 m) (Fig. 2).

Lithology

The mechanic resistance and the permeability of rocks and soils are controlled by the structural and lithologic variations (Champati Ray et al. 2007). Lithology is an essential factor in the landslide zonation (Kayastha et al. 2013). This map is achieved in order to georeference and digitalize the geologic maps 1/50000 covering the study area. Our study area is mainly formed mainly by recent alluvial deposits 7351 ha, marl alternations and limestone marly 4256 ha, sandstone and clay 817 ha, limestone with nummulite 1272 ha, gray marl 1319 ha, triassic facies (gypsum, dolomite) 128 ha, and brown limon 204 ha (Fig. 2).

Distance from the faults

By approaching to the fault, the probability of having landslide increases and becomes more and more important

(Lovine 2008). The map of distance from the faults was prepared by applying the Euclidean distance tools on the faults that were digitalized from the geological map 1/50000, and nine classes were determined (Fig. 2).

Land cover

However, land cover may accelerate the occurrence or play an important role in the occurrence of landslides (Chen and Wang 2007). After a classification of the Sentinel 2 image with ENVI 4.5 by using the maximum likelihood method, four land cover classes were determined; forest, vegetation and agricultural land, built up area, and bare ground. These last levels cover, respectively, 864 ha, 190 ha, 9399 ha, and 4895 ha (Fig. 2).

Methods

In this study, fuzzy logic technique was used to carry out landslide susceptibility mapping. Unlike classical set theory, where an object does or does not belong to a set, in the theory of fuzzy sets, the fuzzy membership values oscillate between 0 and 1, depending on the degree of membership. The problem is that there is no rule on which fuzzy membership values are assigned. Several researchers are simply based on their

subjective judgment, as Bonham-Carter (1994) has shown for mineral exploration, but others are based on statistical analysis (Ercanoglu and Gokceoglu 2002). So the landslide frequency ratio approach was adopted to reduce the subjectivity of this approach. In the one hand, we identify the parameters controlling landslide. It is vitally to anticipate causal factors to predict landslide occurrences because until now there is no universally defined set of factors to predict the spatial occurrences of landslides. Lee and Talib (2005) trust that future landslides will occur under the same conditions as past and present landslides. In the other hand, we calculate the fuzzy membership for each category of each factor. Then, gamma operator was used to integrate the landslide causative factors in order to delineate the landslide susceptibility zones (Fig. 3). Finally, the ROC curve was used to choose the better gamma value to predict areas of high susceptibility to landslides.

Fuzzy membership calculation

Following the hypothesis of Lee and Talib 2005, a relationship can be determined between landslide-related causal factors with landslide occurrences. To quantify this relationship, the frequency ratio can be used. It is the landslide percentage of each land category divided by the area in percent of the same category (Bonham-Carter 1994).

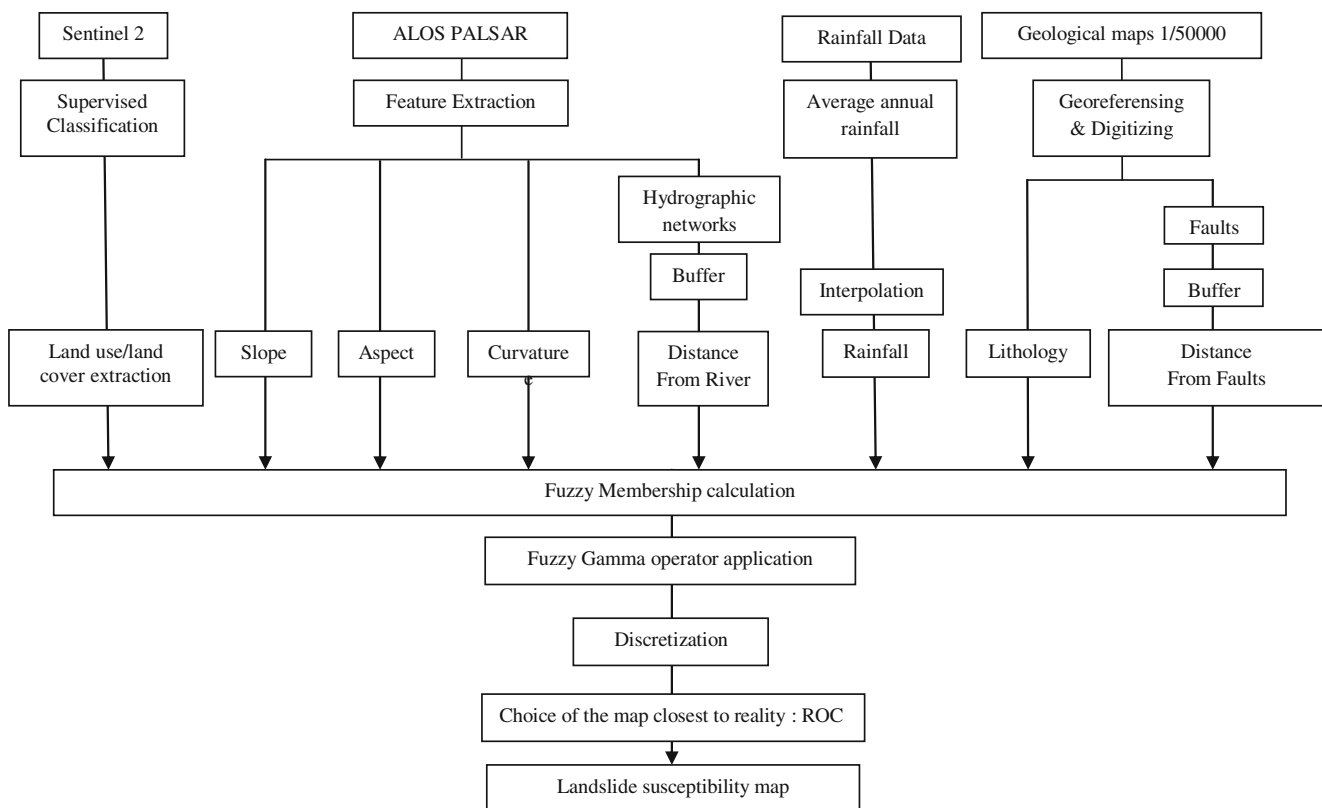


Fig. 3 Methodology organogram for landslides susceptibility mapping

Table 2 Frequency ratio and fuzzy membership values of each parameter

Factors and attributes	Landslide grid %	Total area grid %	Frequency ratio	Membership function
Slope				
0°–5°	0	12	0	0
5°–10°	4.25	32.04	0.13	0.01
10°–15°	44.68	36.76	1.21	0.17
15°–20°	17.02	10.31	1.65	0.24
20°–25°	8.51	5.11	1.66	0.24
> 25°	25.53	3.76	6.78	1
Aspect				
North	27.65	11.26	2.45	0.91
Northwest	36.17	13.48	2.68	1
West	14.89	8.95	1.66	0.62
Southwest	10.63	1.24	1.15	0.42
South	2.12	14.08	0.15	0.05
Southeast	0	18.7	0	0
East	2.12	12.88	0.16	0.06
Northeast	6.38	10.31	0.61	0.23
Flat	0	1.07	0	0
Plan curvature				
(–)	57.44	36.19	1.58	1
0	8.51	25.44	0.33	0.21
(+)	34.04	38.35	0.88	0.55
Profile curvature				
(–)	38.29	39.84	0.96	0.82
0	12.76	17.99	0.7	0.61
(+)	48.93	42.15	1.16	1
Lithology				
Recent alluvial deposits	54.42	47.89	1.13	0.62
Marl alternations and limestone marly	14.96	27.72	0.53	0.29
Sandstone and clay	8.84	5.32	1.66	0.91
Limestone with nummulite	6.12	8.28	0.73	0.40
Gray marl	15.64	8.59	1.82	1
Gypsum and dolomite	0	0.83	0	0
Brown limon	0	1.33	0	0
Distance from fault				
0–150	4.25	5.61	0.75	0.32
150–300	4.25	6.09	0.69	0.29
300–450	0	8.47	0	0
450–600	6.38	12.58	0.5	0.21
600–750	12.76	15.44	0.82	0.34
750–900	48.93	26.57	1.84	0.77
900–1050	6.38	11.49	0.55	0.23
1050–1200	6.38	9.21	0.69	0.29
1200–1350	10.63	4.49	2.36	1

Table 2 (continued)

Factors and attributes	Landslide grid %	Total area grid %	Frequency ratio	Membership function
Rainfall				
< 600	1.17	1.88	0.62	0.53
600–800	10.58	14.72	0.71	0.61
800–1000	31.76	34.76	0.91	0.78
> 1000	56.47	48.62	1.16	1
Distance from river				
0–100	40.42	21.99	1.83	1
100–300	34.04	35.01	0.97	0.52
300–500	14.89	23.26	0.64	0.34
500–800	8.51	16.53	0.51	0.27
> 800	2.12	3.18	0.66	0.36
Land use/land cover				
Forest	2.72	5.63	0.48	0.44
Vegetation and agricultural land	66.66	61.23	1.08	1
Built up area	0.68	1.24	0.54	0.5
Bare ground	29.93	31.89	0.93	0.86

Where

$$FR = \frac{D_i / A_i}{\sum_{i=1}^N D_i / \sum_{i=1}^N A_i} \tag{1}$$

- FR Frequency ratio
- D_i the number of landslide in each category
- A_i the area of each category in each parameter
- N the category number of each parameter

The fuzzy membership follows the principle of conditional probability, if the ratio is equal to 1, so there is a good relationship between landslide and factor classes if the ratio is < 1, so it represents a weak relationship. Normalized value of landslide frequency ratio was used to calculate the fuzzy membership function (Pradhan et al. 2010). Table 2 shows the values of frequency ratio and fuzzy memberships in each factor.

Fuzzy modeling

The theory of fuzzy logic was introduced by Zadeh (1965) as a theory for mathematical modeling where can happen in uncertain conditions. This technique is performed by functions such as OR, AND, SUM, product, and gamma (Bonham and Cox 1995). In this study, we will apply the gamma function due to its rapidity operation and high precision.

The fuzzy gamma operator is the algebraic product of fuzzy product and fuzzy sum, to the power of gamma. The function is as follows:

Table 3 Percentage of susceptibility classes

Gamma value	Area in %				
	Unsusceptible zone	Low susceptibility	Medium susceptibility	High susceptibility	Very high susceptibility
0.75	33.02	27.66	22.41	13.22	3.66
0.85	31.53	17.67	24.93	18.3	7.54
0.90	31.52	14.32	24.9	19.81	9.41
0.92	31.55	12.46	24.11	20.77	11.09

$$\mu c = \left[\prod_{i=1}^n \mu_i \right]^\gamma X \left[1 - \prod_{i=1}^n (1 - \mu_i) \right]^{(1-\gamma)} \tag{2}$$

where γ is a parameter chosen in the range (0, 1).

Results and discussion

We found the highest landslide frequency ratio in the medium slope (10°–15°), therefore we can deduce that slopes with these values are sufficient to trigger a landslide. The rainfall map shows an average annual rainfall of > 1000 mm with the highest value of frequency ratio (1.16) indicating the highest probability of landslide occurrence in this class. The topographic aspect is equally considered as an important factor in this research. The level of very high frequency ratio 2.45 and 2.68 is found respectively in the north and northwest because they receive the highest rainfall. The map of distance from river indicates that frequency ratio of the range of 0–100 m and 100–300 m is revealed to be high in the buffer drainage case, and it could be attributed to stream bank erosion which leads to landslides. Each geological formation is characterized by a lithology which could run landslide incidence. By analyzing the frequency ratio results of geology layer, we found that the recent alluvial deposits are the most susceptible to landslide in view of their fragility (clays and ancient soils) but the highest frequency ratio value is found in gray marl because it has a value of landslide frequency that is almost twice its area. Within the land use classes, we noticed a high value of landslide frequency in vegetation and agricultural land. The highest landslide frequency ratio was observed in the negative values of plan curvature. But in the case of profile curvature, the highest value of frequency ratio was

Table 4 AUC of different gamma values

Gamma value	Area under curve
0.75	0.885
0.85	0.865
0.90	0.89
0.92	0.877

observed in the positive values. We found 8.51% of the landslides in class 0 (curvate plan) and 12.76% in class 0 of the curvate profile because these areas have a certain inclination (the slope) which can trigger some landslides. Therefore it can be concluded that concave slopes always occupy the maximum of landslides. About distance from the faults, the highest frequency ratio was found in the last range with a value of 2.36. This is explained by the stability of this zone. Four landslides susceptibility maps were developed applying four different gamma values (0.75, 0.85, 0.90, and 0.92). Until now, landslide susceptibility values are represented by a continuous data. To better visualize the results, we applied a discretization. Data discretization remains uncertain in landslide susceptibility mapping (Kritikos and Davies 2011). Therefore, most researchers use their expert opinion to delineate classes (Ayalew et al. 2004; Kritikos and Davies 2011). In our study, a discretization based on Jenks natural breaks classification method was performed, because it reduces the variance within classes and maximizes the variance between classes. So, landslide susceptibility maps were divided into five classes (no susceptibility, low susceptibility, medium susceptibility, high susceptibility, and very high susceptibility). Landslide susceptibility maps show that the spatial distribution of susceptibility classes varies from one map to another. Table 3 shows the percentage occupied by the susceptibility areas for different gamma values.

For example, in the case of γ (0.75), 33.02% of the area was occupied by unsusceptible area, and 27.66% was located in low susceptible area, 22.41% in medium susceptible area, 13.22% in high susceptible area, and 3.66% in very high susceptible area. But in γ (0.90), 31.54% of the area was occupied by unsusceptible area, and 14.32% was located in low

Table 5 Landslides distribution

Landslides susceptibility	Number of landslides
Non susceptible zone	1
Low susceptible zone	7
Moderate susceptible zone	28
High susceptible zone	44
Very high susceptible zone	67

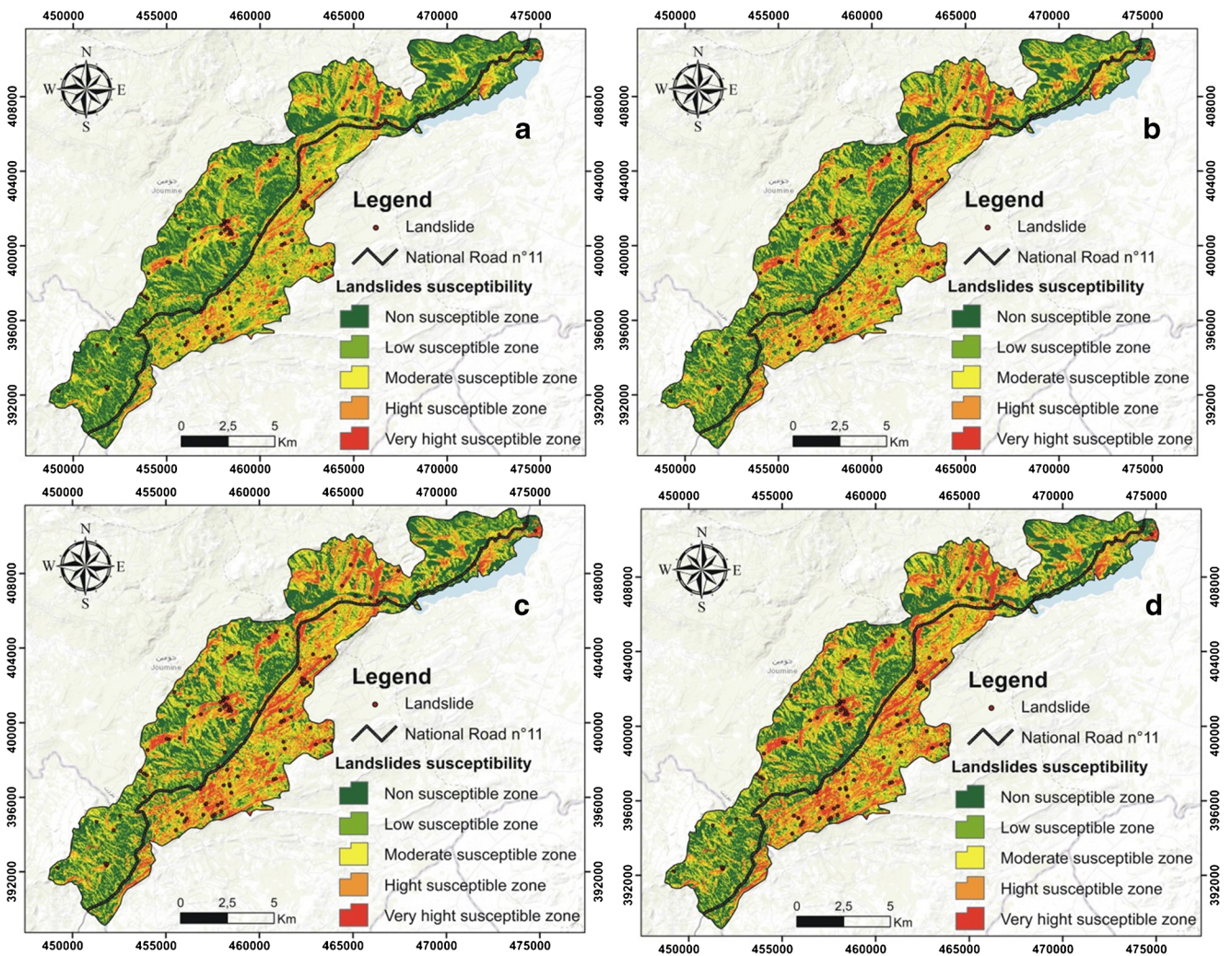


Fig. 4 Landslide susceptibility map for different γ values, (A) 0.75, (B) 0.85, (C) 0.90, and (D) 0.92

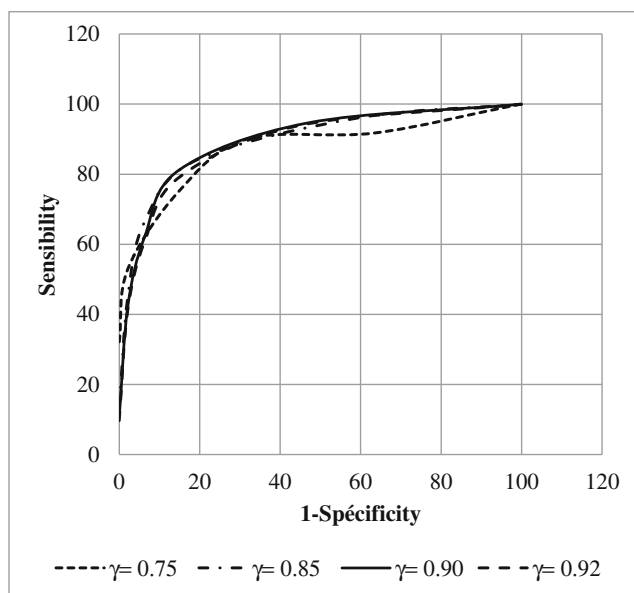


Fig. 5 The ROC graph of different gamma cases

susceptible area, 24.9% in medium susceptible area, 19.81% in high susceptible area, and 9.41% in very high susceptible area.

To choose the map closest to reality, the receiver operating curves characteristic (ROC) has been applied.

Choice and validation of landslide susceptibility map

The receiver operating characteristic is often represented as a curve that gives the sensitivity (landslides that are actually detected) as a function of the specificity (stable areas that are incorrectly detected). Sensitivity represents the probability to have a slipped cell in the correct class, and it is shown on the y-axis in a ROC curve. But, 1-specificity is the false positive rate, and it is taken along the x-axis of the curve. The reliability of this method is tested by the area under curve (AUC) (Williams et al. 1999). A perfect test has an AUC equal to 1, while an AUC of 0.5 represents a weak test.

By examining the results of the ROC curve, we find that gamma 0.90 has the highest value of AUC (0.89). The case of gamma 0.75 has the lowest value of AUC (0.865) (see Table 4, Fig. 5).

Finally, the gamma value of 0.90 was chosen. Figure 4c shows the distribution of different susceptibility zones after discretization. The northwest-facing slopes are more susceptible to landslides than those facing to south, and they contain 98 landslides because they are the most humid. The high susceptibility area is found in the proximity of drainages and bare ground. The highest susceptible zones are found near the high slopes exposed to the north, cliffs, and cut slopes adjoining the roads. Low susceptibility zones are observed in the agricultural area, the forests, and the low slopes exposed essentially to the south and the southeast. Without validation, the prediction model will have no scientific significance (Chung and Fabbri 2003; Bui et al. 2011). The validation of landslide susceptibility model is done after verification of the predictive capacities of the landslide susceptibility map. There are two types of error found in landslide susceptibility map. Landslide scan occurs in stable areas and the can be absent in unstable areas (Soeters and van Westen 1996). In our case study, the prediction accuracy of landslide susceptibility map was evaluated on the basis of an expert evaluation method using known landslide locations (Pradhan 2010). A good quality map must predict the most of the landslides in the high or very high susceptibility class, in contrast to the low or negligible susceptibility class. In addition to that, the different classes must be composed by agglomerated pixels and avoid the “isolated pixel” effect (Table 5).

By examining the spatial distribution of landslides in the susceptibility map of gamma 0.9, we distinguish that the non-susceptible zone and the low susceptible zone contain together eight landslides. However, high and very high susceptible zone contains 111 landslides.

Conclusion

To minimize the subjectivity of fuzzy logic method, the frequency ratio was used. The using of fuzzy gamma operator to map landslide susceptibility has achieved acceptable result. Gamma 0.90 has the highest AUC with 0.89. The model proves that gamma 0.90 shows the better prediction of landslides susceptibility mapping. By examining the spatial distribution of landslides, we can say that landslides susceptibility mapping using the frequency ratio and the fuzzy logic with gamma value 0.90 is efficient to predict the landslides susceptibility in our study area with a reliability of 89%.

References

- Ayalew L, Yamagishi H (2005) The application of GIS-based logistic regression for landslide susceptibility mapping in the Kakuda–Yahiko Mountains, Central Japan. *Geomorphology* 65(1/2):15–31
- Ayalew L, Yamagishi H, Ugawa N (2004) Landslide susceptibility mapping using GIS-based weighted linear combination, the case in Tsugawa area of Agano River, Niigata Prefecture, Japan. *Landslides* 1(1):73–81. <https://doi.org/10.1007/s10346-003-0006-9>
- Bnovallot J (1984a) Glissement de terrain et aménagement du milieu naturel dans une montagne méditerranéenne humide. Le cas des Atafas, Kroumirie, Tunisie septentrionale. Le développement rural en question, Ed ORSTOM:29–54
- Bnovallot J (1984b) Population, occupation du sol et mouvements de masses dans la région d’Ain Draham (Tunisie septentrionale). Communication du colloque Mouvements de terrains, Caen, série documents du BRGM 83:609–618
- Bonham C, Cox S (1995) *Econ Geol* 90:1352
- Bonham-Carter GF (1994) Geographic information systems for geoscientists: modeling with GIS. New York. Pergamon/Elsevier, Ottawa, p 398
- Bui DT, Lofman O, Revhaug I, Dick O (2011) Landslide susceptibility analysis in the Hoa Binh province of Vietnam using statistical index and logistic regression. *Nat Hazards* 59(3):1413–1444
- Carrara AM, Cardinali R, Detti F, Guzzetti VP, Reichenbach P (1991) GIS techniques and statistical models in evaluating landslide hazard. *Earth Surf Process Landf* 16:427–445
- Champati Ray PK, Dimri S, Lakhera RC, Sati S (2007) Fuzzy-based method for landslide hazard assessment in active seismic zone of Himalaya. *Landslides* 4:101–111
- Chen Z, Wang J (2007) Landslide hazard mapping using logistic regression model in Mackenzie Valley, Canada. *Natural Hazards* 42(1): 75–89. <https://doi.org/10.1007/s11069-006-9061-6>
- Chung CJF, Fabbri AG (2003) Validation of spatial prediction models for landslide hazard mapping. *Nat Hazards* 30(3):451–472
- Dahal RK, Hasegawa S, Yamanaka M, Dhakal S, Bhandary NP, Yatabe R (2009) Comparative analysis of contributing parameters for rainfall-triggered landslides in the lesser Himalaya of Nepal. *Environ Geol* 58(3):567–586
- Das I, Sahoo S, van Westen C, Stein A, Hack R (2010) Landslide susceptibility assessment using logistic regression and its comparison with a rock mass classification system, along a road section in the northern Himalayas (India). *Geomorphology* 114:627–637
- DeGraff J, Romesburg H (1980) Regional landslide susceptibility assessment for wildland management: a matrix approach. In: Coates D, Vitek J (eds) *Thresholds : Geomorphology* George Allen and Unwin, London, pp 401–414
- Demoulin A, Chung CF (2007) Mapping landslide susceptibility from small datasets: a case study in the Pays de Herve (E Belgium). *Geomorphology* 89:391–404
- EL Aroui O (2016) Géomorphologie des mouvements de terrain en Kroumirie septentrionale (Tunisie). Edition Faculté des Lettres, des Arts et des Humanités de la Manouba (Tunisie) 356 p.
- El Aroui O (2017) Etude et cartographie des mouvements de terrain sur les versants du synclinal perché de Dyr El Kef (Tunisie du nord-ouest). *Revue Tunisienne de Géographie* 46-74:87–109
- Ercanoglu M, Gokceoglu C (2002) Assessment of landslide susceptibility for a landslide-prone area (north of Yenice, NW Turkey) by fuzzy approach. *Environ Geol* 41:720–730
- Ercanoglu M, Gokceoglu C (2004) Use of fuzzy relations to produce landslide susceptibility map of a landslide prone area (West Black Sea region, Turkey). *Eng Geol* 75(3–4):229–250
- Feizizadeh B, Blaschke T (2012a) Uncertainty and decision strategy analysis of GIS-based ordered weighted averaging method for landslide

- susceptibility mapping in Urmia lake basin, Iran. Proceedings of the International Conference of GI Science, Columbus
- Feizizadeh B, Blaschke T (2012b) Land suitability analysis for Tabriz County, Iran: a multi-criteria evaluation approach using GIS. *J Environ Plan Manag* 56:1–23
- Feizizadeh B, Blaschke T, Nazmfar H (2012) GIS-based ordered weighted averaging and Dempster-Shafer methods for landslide susceptibility mapping in Urmia lake basin, Iran. *Int J Digit Earth* 7:688–708
- Gupta RP, Kanungo DP, Arora MK, Sarkar S (2008) Approaches for comparative evaluation of raster GIS-based landslide susceptibility zonation maps. *Int J App Earth Obs Geoinform* 10:330–341
- Ilanloo M (2011) A comparative study of fuzzy logic approach for landslide susceptibility mapping using GIS: An experience of Karaj dam basin in Iran. *Procedia - Social and Behavioral Sciences* 19:668–676
- Intarawichian N, Dasananda S (2010) Analytical hierarchy process for landslide susceptibility mapping in lower Mae Chem watershed, northern Thailand Suranaree. *J Sci Technol* 17(3):277–292
- Jordan C, O'Connor E, Marchant A, Northmore A, Greenbaum D, McDonald A, Kovacic M, Ahmed R (2000) Rapid landslide susceptibility mapping using remote sensing and GIS modelling. Proc: In 14th International Conference on Applied Geologic Remote Sensing, Las Vegas: 113–120
- Kanungo DP, Arora MK, Sarkar S, Gupta RP (2006) A comparative study of conventional, ANN black box, fuzzy and combined neural and fuzzy weighting procedures for landslide susceptibility zonation in Darjeeling Himalayas. *Eng Geol* 85:347–366
- Kanungo DP, Arora MK, Sarkar S, Gupta RP (2009) A fuzzy set based approach for integration of thematic maps for landslide susceptibility zonation. *Georisk* 3(1):30–43
- Kayastha P, Dhital MR, De Smedt F (2013) Application of the analytical hierarchy process (AHP) for landslide susceptibility mapping: a case study from the Tinau watershed, West Nepal. *Comput Geosci* 52: 398–408
- Krejci O, Baron I, Bil M, Hubatka F, Jurova Z, Kirchner K (2002) Slope movements in the Flysch Carpathians of Eastern Czech Republic triggered by extreme rainfalls in 1997: a case study. *Phys Chem Earth* 27:1567–1576
- Kritikos T, Davies TRH (2011) GIS-based multi-criteria decision analysis for landslide susceptibility mapping at northern Evia, Greece. *Z dt Ges Geowiss* 162:421–434
- Lee S, Talib JA (2005) Probabilistic landslide susceptibility and factor effect analysis. *Environ Geol* 47:982–990
- Lovine G (2008) Mud-flow and lava-flow susceptibility and hazard mapping through numerical modelling, GIS techniques, historical and geo-environmental analyses. In Proceedings of the iEMSs 4th biennial meeting, international congress on environmental modelling ANS software: integrating sciences and information technology for environmental assessment and decision making vol 3 :1447–1460
- Marston R, Miller M, Devkota L (1998) Geoecology and mass movements in the Manaslu Ganesh and Langtang-Jural Himal, Nepal. *Geomorphology* 26:139–150
- Marthelot P (1957) L'érosion dans la montagne Kroumir. *Revue de géographie alpine* 45(2):273–287
- Marthelot P, (1959) Note sur un décollement de versant dans la vallée des Atafra (Kroumirie). Actes du 84^e congr. Nat. Suc. Sav., Dijon 1959. Section de Geographic : 61–65.
- Nagarajan R, Mukherjee A, Roy A, Khire MV (1998) Temporal remote sensing data and GIS application in landslide hazard zonation of part of Western Ghat, India. *Int J Rem Sens* 19(4):573–585
- Nefeslioglu HA, Duman TY, Durmaz S (2008) Landslide susceptibility mapping for a part of tectonic Kelkit Valley (Eastern Black Sea region of Turkey). *Geomorphology* 94:401–418
- Parise M (2001) Landslide hazard zonation of slopes susceptible to rock falls and topples. *Nat Hazards Earth Syst Sci* 2:37–49
- Pourghasemi HR, Moradi HR, Fatemi A, Said M, Mahdavi MR, Mohammadi R (2009) Landslide hazard assessment using fuzzy multi criteria decision-making method. *Iran J Watershed Manag Sci Eng* 3(8):51–62
- Pradhan B (2010) Application of an advanced fuzzy logic model for landslide susceptibility analysis. *Int J Comput Intel Sys* 3(3):370–381
- Pradhan B, Lee S, Buchroithner M (2010) Remote sensing and GIS-based landslide susceptibility analysis and its cross-validation in three test areas using a frequency ratio model. *Photogram Fernerkundung Geolnf* 1:17–32
- Saha AK, Gupta RP, Arora MK (2002) GIS-based landslide hazard zonation in a part of the Himalayas. *Int J Rem Sens* 23(2):357–369
- Soeters R, van Westen CJ (1996) Slope instability recognition analysis and zonation. In: Turner KT, Schuster RL (eds) Landslides. Investigation and mitigation, special report no. 247. Transportation Research Board National Research Council, Washington DC, pp 129–177
- Van Westen CJ (1993) Application of geographic information systems to landslide hazard zonation. ITC publication no 15, International Institute for Aerospace and Earth Resources Survey, Enschede, The Netherlands, 245.
- Williams CJ, Lee SS, Fisher RA, Dickerman LH (1999) A comparison of statistical methods for prenatal screening for Down syndrome. *Appl Stoch Model Data Anal* 15:89–101
- Wu Y, Li W, Wang Q, Liu Q, Yang D, Xing m, Pei Y, Yan S (2016) Landslide susceptibility assessment using frequency ratio, statistical index and certainty factor models for the Gangu County, China. *Arabian Journal of Geosciences* 9(2)
- Yalcin A, Reis S, Aydinoglu AC, Yomralioglu T (2011) A GIS-based comparative study of frequency ratio, analytical hierarchy process, bivariate statistics and logistics regression methods for landslide susceptibility mapping in Trabzon, NE Turkey. *CATENA* 85(3): 274–287
- Zadeh LA (1965) *Inf Control Thesis*. 8:38